Check for updates

EARTH SURFACE PROCESSES AND LANDFORMS
Earth Surf. Process. Landforms **45**, 2927–2939 (2020)
© 2020 John Wiley & Sons, Ltd.
Published online 16 July 2020 in Wiley Online Library
(wileyonlinelibrary.com) DOI: 10.1002/esp.4940

The effects of longitudinal variations in valley geometry and wood load on flood response

Sarah Hinshaw,[1] Ellen Wohl[1]* and Dany Davis[2]
[1] Department of Geosciences, Colorado State University, Fort Collins, CO 80523-1482, USA
[2] New York City Department of Environmental Protection, Flushing, NY 11373, USA

Received 22 November 2019; Revised 8 June 2020; Accepted 10 June 2020

*Correspondence to: Ellen Wohl, Department of Geosciences, Colorado State University, Fort Collins, CO 80523-1482, USA. E-mail: ellen.wohl@colostate.edu

ESPL
Earth Surface Processes and Landforms

ABSTRACT: We use field measurements and airborne LiDAR data to quantify the potential effects of valley geometry and large wood on channel erosional and depositional response to a large flood (estimated 150-year recurrence interval) in 2011 along a mountain stream. Topographic data along 3 km of Biscuit Brook in the Catskill Mountains, New York, USA reveal repeated downstream alternations between steep, narrow bedrock reaches and alluvial reaches that retain large wood, with wood loads as high as 1261 m^3 ha^{-1}. We hypothesized that, within alluvial reaches, geomorphic response to the flood, in the form of changes in bed elevation, net volume of sediment eroded or aggraded, and grain size, correlates with wood load. We hypothesized that greater wood load corresponds to lower modelled average velocity and less channel-bed erosion during the flood, and finer median bed grain size and a lower gradation coefficient of bed sediment. The results partly support this hypothesis. Wood results in lower reach-average modelled velocity for the 2011 flood, but the magnitude of change in channel-bed elevation after the 2011 flood among alluvial and bedrock reaches does not correlate with wood load. Wood load does correlate with changes in sediment volume and bed substrate, with finer grain size and smaller sediment gradation in reaches with more wood. The proportion of wood in jams is a stronger predictor of bed grain-size characteristics than is total wood load. We also see evidence of a threshold: greater wood load correlates with channel aggradation at wood loads exceeding approximately 200 m^3 ha^{-1}. In this mountain stream, abundant large wood in channel reaches with alluvial substrate creates lower velocity that results in finer bed material and, when wood load exceeds a threshold, reach scale increases in aggradation. This suggests that reintroducing small amounts of wood or one logjam for river restoration will have limited geomorphic effects. © 2020 John Wiley & Sons, Ltd.

KEYWORDS: large wood; logjam; bedrock channel; sediment storage

Introduction

Rivers in high-relief terrain commonly alternate downstream between valley segments with steep, laterally confined, predominantly bedrock channels and lower-gradient, wider, alluvial reaches (Wohl, 2010). Longitudinal variations in valley-bottom geometry correspond to variations in peak flow attenuation; stream power; storage of sediment, particulate organic matter, and large wood; biogeochemical processing; and habitat abundance and diversity (Stanford *et al.*, 1996; Wohl and Cadol, 2011; Bellmore and Baxter, 2014; Hauer *et al.*, 2016; Venarsky *et al.*, 2018; Wohl *et al.*, 2018a). Consequently, understanding the spatial patterns of these variations can provide insight into river response to disturbances such as floods by identifying reaches that are most geomorphically or ecologically resilient to change during floods. In reaches with large wood, individual pieces or accumulations of wood can mediate response to floods by creating obstructions to flow that influence the spatial distribution of hydraulic forces (e.g. Gippel, 1995).

Values of wood load (volume of wood per unit area of valley bottom) in many streams are higher in wide, low-gradient reaches because of reduced transport capacity relative to steep, narrow reaches with similar drainage area (e.g. Wohl and Cadol, 2011; Rigon *et al.*, 2012; Wyzga *et al.*, 2017). Individual wood pieces and jams within the channel and floodplain in wider reaches also have the potential to create feedbacks in which the additional hydraulic roughness and flow obstruction created by wood enhance hyporheic exchange flows and associated biogeochemical processes (Sawyer *et al.*, 2011; Sawyer and Cardenas, 2012); lower local and reach-averaged velocity (Shields and Smith, 1992; Manners *et al.*, 2007) and associated sediment retention and range of the bed-material size distribution (Montgomery *et al.*, 1996; Buffington and Montgomery, 1999; Rigon *et al.*, 2012; Wohl and Scott, 2017); and formation of secondary channels (Sear *et al.*, 2010; Wohl, 2011; Collins *et al.*, 2012). Wider reaches can thus enhance storage of large wood, and wood in storage can facilitate development of complex channel and floodplain morphology (e.g. bars and secondary channels) that may further enhance storage potential for large wood (Wohl *et al.*, 2018b). Interactions between channel geometry, sediment dynamics, and large wood storage in the wider reaches can enhance river resilience to disturbance by attenuating downstream fluxes of water, solutes, sediment, and organic matter (Wohl *et al.*, 2018a).

Comiti *et al.*'s (2016) review of large wood recruitment and transport during large floods summarizes the limited number of studies on the topic. Most of these studies come from catchments in the European Alps, but a few have been conducted in the western United States. As might be expected, there is substantial catchment-specific variability in wood recruitment and transport during floods, with dominant recruitment source depending on the extent of channel widening and hillslope–channel connectivity for large wood. Large wood transport mostly occurs under supply-limited conditions. Wood deposition in the European streams occurs primarily at bridges. In channels with less infrastructure, floods tend to increase wood load in smaller (second-order) channels and redistribute wood in larger channels, with preferential deposition in jams and on bars (e.g. Marcus *et al.*, 2002) and at wider, lower-gradient sites (e.g. Swanson *et al.*, 1998; Ruiz-Villanueva *et al.*, 2018). Large wood in transport can also batter riparian vegetation along the channel margins, causing additional wood recruitment during a large flood (Johnson *et al.*, 2000).

Despite an extensive literature on large wood in river corridors, few studies provide detailed examinations of how wood interacts with valley geometry, discharge, and sediment supply to influence river corridor response to an extreme flood. Here, we use Biscuit Brook in the Catskill Mountains of New York, USA to examine these interactions based on LiDAR surveys prior to and following an extreme flood in 2011. Specifically, we evaluate the potential influence of large wood on channel response during the August 2011 flooding associated with Hurricane Irene. This flood has been estimated as having a 150-year recurrence interval at the study site. Studies in other catchments affected by this flood indicate that the storm initiated and reactivated many landslides that recruited substantial volumes of sediment (Magilligan *et al.*, 2015) and large wood to stream channels, especially in small upland catchments analogous to Biscuit Brook. In small upland catchments, enhanced wood recruitment resulted in formation of logjams (Dethier *et al.*, 2016).

Biscuit Brook has pronounced longitudinal variations between incised bedrock reaches and alluvial reaches with substantial wood loads. We start from the observation that valley geometry sets the macro template for channel response because the downstream alternation between bedrock and alluvial reaches corresponds to differences in lithology. Bedrock reaches along Biscuit Brook occur primarily in association with sandstone. These reaches exhibit a downstream progression from relatively planar channel morphology to parallel longitudinal grooves to a pronounced inner channel (see Figure S1 in the online Supporting Information). Downstream from the inner channel, where the channel widens again, planar bedrock along the valley bottom is swept clear of sediment and vertical bedrock walls are present at the valley margins. In contrast, a gently sloping, soil-mantled valley side wall grades into the valley bottom in alluvial reaches (Figure S1).

Similar reach-scale progression in bedrock erosional forms has been described for persistent knickzones in flume experiments (Wohl and Ikeda, 1997) and natural channels (Wohl, 1993). The presence of this longitudinal sequence in bedrock reaches of Biscuit Brook suggests that exposure of bedrock along the channel is persistent rather than transient. Persistent bedrock exposure indicates that transport capacity exceeds sediment supply, in contrast to alluvial reaches along Biscuit Brook.

Our primary objective is to quantify longitudinal patterns of channel morphology and the potential effects of valley geometry and large wood on channel response to the 2011 flood. We hypothesized that, within alluvial reaches, geomorphic response to the flood would correlate with wood load. Geomorphic response refers to changes in bed elevation, net volume of sediment eroded or aggraded, and bed grain size. We hypothesized that greater wood load corresponds to lower modelled average velocity during the flood, less net channel-bed erosion during the flood, and finer median bed grain size and a lower gradation coefficient of bed sediment. Because this is an observational field study, rather than a manipulative experiment, we cannot remove potential effects on local flood response associated with other factors such as sediment source location, nor eliminate the correlation of wood load with channel morphology. We use statistical analyses to examine the relative influences of multiple potential controls on flood response.

Previous studies in canyon rivers demonstrate that channel response to floods reflects valley geometry (e.g. Shroba *et al.*, 1979; Wohl, 1992; Righini *et al.*, 2017) such that less laterally confined and lower-gradient reaches experience primarily net deposition during floods, whereas the high transport capacity of narrow, steep reaches results in erosion and transport during floods. Our distinctive contribution is to examine the role of large wood in mediating geomorphic response to a large flood within alluvial reaches of a stream and to evaluate the effects of wood load and spatial concentration of wood in jams on channel response.

Study Area

Biscuit Brook drains 10.7 km^2 within the larger watershed of the Neversink River in the Catskill Mountains of New York, USA (Figure 1). The watershed is underlain by Devonian-age undeformed sedimentary rocks of the Walton Formation (Ver Straeten, 2013) comprising a repeating sequence of fluvial sandstones/siltstones and paleo-floodplain shales/mudstones. Sandstone that is relatively resistant to erosion alternates longitudinally with weaker mudstone along the channel of Biscuit Brook: the wide, low-gradient valley segments are commonly associated with the presence of mudstone at river level. The bedrock is variably mantled by Pleistocene glacial deposits including consolidated lodgement till, ground moraine till, and kame terrace unconsolidated deposits that form valley-side slopes and valley-bottom terraces. Erosion into the glacial sediment is a source of Biscuit Brook alluvium.

Elevation drops from 1130 m at the drainage divide to 610 m at the outlet. Average annual precipitation of 1420 mm is spread evenly throughout the year, including winter snowfall. Eastern deciduous forest dominated by American beech (*Fagus grandifolia*), yellow birch (*Betula alleghaniensis*), eastern hemlock (*Tsuga canadensis*), striped maple (*Acer pensylvanicum*), and sugar maple (*Acer saccharum*) covers the watershed.

A stream gauge has been present at the downstream end of the Biscuit Brook watershed since 1983 (USGS 01434025). Average daily discharge for the period of record through 2018 is 0.45 $m^3\ s^{-1}$ and the 2-year recurrence interval flow is 8.98 $m^3\ s^{-1}$. In late August 2011, Hurricane Irene delivered extreme rainfall to the Catskill region around Biscuit Brook, with up to 268–292 mm over 24 h. This produced floods of record for all stream gauges in the upper Neversink River basin (Lumia *et al.*, 2014). The US Geological Survey estimated a peak discharge of 42 $m^3\ s^{-1}$ at the damaged Biscuit Brook gauge. This corresponds to a recurrence interval of ~150 years based on a log-Pearson Type III distribution using the annual maximum peak series for the period 1984–2018 and regionalized skew coefficients. Hurricane Irene flood recurrence intervals for the most part ranged from 50 to 500+ years throughout

© 2020 John Wiley & Sons, Ltd.

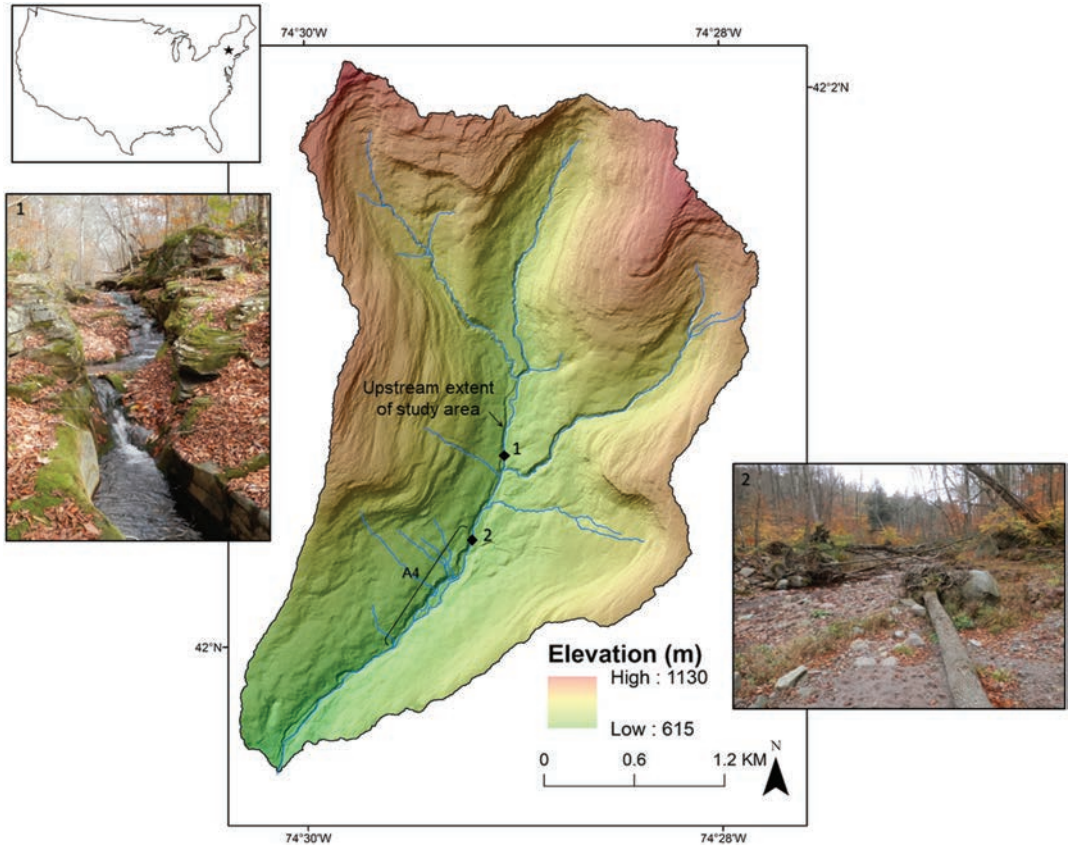

FIGURE 1. Location map of the study area, indicating the location of the Biscuit Brook watershed within the continental United States, and illustrating representative bedrock (1) and alluvial (2) reaches in the inset photos. The upstream extent of the study area and the location of reach A4 are shown on the map. The downstream extent of the study area is the bottom of the watershed. [Colour figure can be viewed at wileyonlinelibrary.com]

the eastern Catskill Mountains, similar in magnitude to Hurricane Irene flooding in the Green Mountains of Vermont (Yellen *et al.*, 2014; Dethier *et al.*, 2016). Digital elevation models (DEMs) with ~1 m resolution were developed from airborne LiDAR flown over the watershed in 2009 and 2013–14, allowing us to evaluate change in the river corridor during the period that included Hurricane Irene, as detailed in the Methods section.

Biscuit Brook within the study area is undeveloped, with access only by a foot-trail. Wood is recruited to the river corridor via individual tree fall, mass tree mortality – primarily via landslides and windstorms – and to a lesser extent ice storms, bank erosion, and fluvial transport from tributaries and upstream portions of the mainstem. Field observations suggest that individual tree mortality and bank erosion are the dominant sources of large wood in the river corridor, although mass tree mortality from microburst wind events has occurred in the Catskills and we observed recent scars from landslides that introduced trees to the river corridor. Hemlock trees (*Tsuga* spp.) are also currently undergoing widespread die-off in the Catskills as a result of the invasive hemlock woolly adelgid insect (*Adelges tsugae*) (Yorks *et al.*, 2000), as are ash trees (*Fraxinus* spp.) as a result of the invasive emerald ash borer (*Agrilus planipennis*).

Methods

Field measurements

The portion of Biscuit Brook surveyed during summer 2018 is 3050 m in length as measured along the active channel. We divided this length into 16 reaches. Each reach was delineated in the field based on longitudinally consistent channel and valley morphology. Each reach was designated as having predominantly bedrock (8 reaches) or predominantly alluvial (8 reaches) channel substrate. The valley geometry of each reach was extracted from the 2014 DEM. Table 1 lists characteristics of the reaches, which are numbered sequentially downstream from reach A1.

We mapped all wood greater than 10 cm in diameter and 1 m in length within the bankfull channel. Jams were defined as three or more pieces in contact. We mapped the location of all pieces and jams using a handheld Garmin GPSmap 62stc (±3 m horizontal accuracy) and visually identified evidence of geomorphic influence (sediment storage upstream, scour downstream, redirection of flow). We measured the length and average diameter of each wood piece, and the length, width, and height of each jam.

Reach A4 (alluvial), which is the longest reach at 885 m, was further divided into eight subreaches because of its length, diversity of morphologic features, and substantial longitudinal variation in wood load (Figure 2, Table 1). In particular, this reach included a subreach in which the channel became poorly defined, with low to non-existent banks and split flow, suggesting extreme local aggradation. Field-delineated subreach boundaries were overlaid on a raster created from the difference between the 2009 and 2014 DEMs for preliminary identification of storage and transport zones within reach A4 during the period that included Hurricane Irene.

We surveyed 57 cross-sections and the channel gradient in A4 using either an autolevel or laser rangefinder (TruPulse 360B, ±0.1 m resolution) with a metric tape and stadia rod. In subreaches with substantial large wood accumulations,

© 2020 John Wiley & Sons, Ltd.

Table 1. Characteristics of the study reaches and the subreaches within A4

Reach	Reach L (m)	VB w (m)	S (mm^{-1})	LW load (m^3 ha^{-1})	Avg ΔE (m), 2009–14	Avg Δvol (m^3), 2009–14	Avg 1-y v (ms^{-1})	Avg 2011 v (ms^{-1})
A1	126	17	0.03	370	−0.09	−193	2.48	5.02
B1	126	12	0.06	0	−0.22	−353	2.82	6.40
A2	55	11	0.05	546	−0.12	−71	3.05	6.38
B2	104	13	0.05	0	−0.35	−461	2.70	5.79
A3	227	20	0.03	23	−0.42	−1908	2.41	5.23
B3	80	16	0.05	0	−0.96	−1246	3.10	5.69
A4	885	44	0.03	485	−0.12	323[1]	2.03	3.91
A4a	82	25	0.04	0	−1.19	−2397	1.84	4.79
A4b	66	30	0.04	487	−0.84	−1697	2.39	5.11
A4c	96	23	0.03	4	−0.04	−95	2.17	4.66
A4d	111	27	0.02	9	0.58	1722	1.98	3.60
A4e	191	46	0.04	1261	0.55	4819	2.28	3.79
A4f	126	77	0.03	108	0.04	381	2.16	3.55
A4g	91	71	0.03	760	0.14	912	1.18	2.35
A4h	122	52	0.04	264	−0.17	−1059	2.21	3.43
B4	27	16	0.03	0	−0.43	−189	2.43	4.17
A5	215	27	0.02	111	0.09	515	1.96	3.60
B5	315	17	0.03	0	−0.32	−1717	2.65	5.23
A6	137	34	0.05	0	−0.11	−533	2.28	4.57
B6	498	14	0.03	0	−0.20	−1411	2.25	4.49
A7	133	39	0.04	90	0.12	625	2.25	4.24
B7	47	17	0.03	0	−0.01	−4	1.96	4.41
A8	21	16	0.02	0	−0.15	−50	1.92	4.48
B8	54	24	0.02	0	0.07	97	1.86	4.37

A refers to an alluvial reach and B to a bedrock reach. Reach L is reach length; VB w is valley-bottom width; S is average channel gradient; LW load is total wood load, with area derived from reach length and average effective valley width; avg ΔE is average bed-elevation change between two LiDAR surveys; avg Δ vol is average net volume of erosion (negative) or aggradation (positive) between two LIDAR surveys; avg 1-y v is modelled average velocity for a discharge of 4.5 m^3 s^{-1} with large wood included; avg 2011 v is modelled average velocity for the 2011 flood with large wood included.
[1]Volume change for A4 is based on the sum of subreach values.

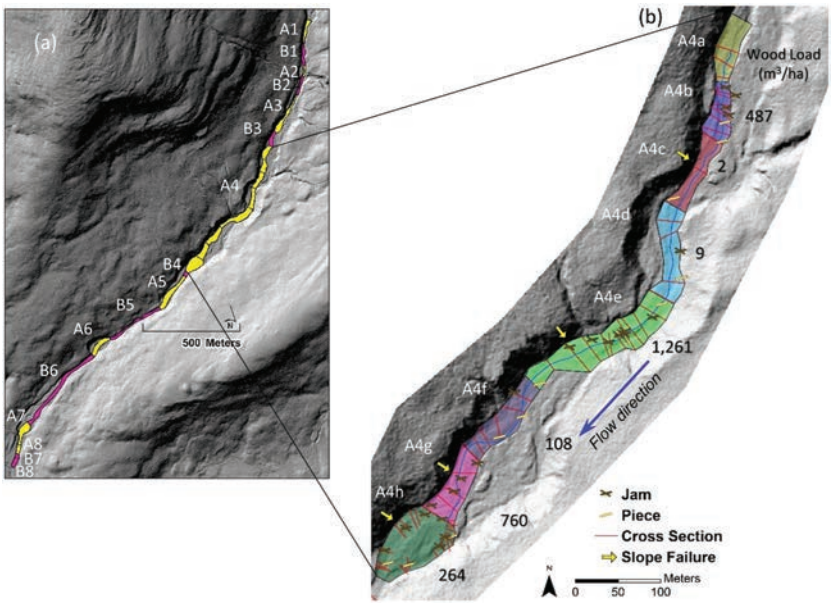

FIGURE 2. Longitudinal distribution of alluvial (yellow) and bedrock (pink) reaches within the Biscuit Brook study area. Detailed map indicates longitudinal distribution of subreaches within reach A4. Red lines indicate surveyed cross-sections and yellow bars indicate mapped large wood. [Colour figure can be viewed at wileyonlinelibrary.com]

cross-sections were located upstream, over (with points on the logjam and on the underlying channel surface), and downstream from logjams in order to capture the effects of wood on channel geometry. We conducted 19 clast counts of bed surface substrate in reach A4. Each count included 100 clasts chosen via random walk and measured with a gravelometer. Clast measurement sites were distributed at regular intervals longitudinally along a metric tape laid down the centre of the main channel and, where present, secondary channels. Sediment size distributions were obtained by grouping measurement sites within each subreach. We noted the location of hillslope failures using the handheld GPS and measured the surface area of each failure using a laser rangefinder. We noted the location and size of hillslope failures in order to evaluate whether the location of alluvial versus bedrock reaches corresponds to differing relative amounts of sediment

© 2020 John Wiley & Sons, Ltd.

Table 2. Variables used in analyses of reach A4. Bold variables passed model selection criteria for single or multiple linear regression

Variable	Method of calculation	Source (reference)
Grain size (D_{50})	Grain size analysis spreadsheet	Field data (Pontyondy and Bunte, 2002)
Gradation coefficient	$\sigma_g = \left(\frac{d_{84}}{d_{16}}\right)^{\frac{1}{2}}$	Field data (Julien, 2010)
Slope (S)	Average of three iterations, slope of linear regression of elevation, and distance in each reach	Interpolate line tool, GIS 10.5.1
Bedrock proportion (Br)	Percentage of bedrock present during pebble counts	Wolman (1954)
Geologic valley width (W_v)	Visually defined in GIS with clear bedrock valley boundaries	2013 DEM, NYCDEP
Effective valley width (W_{ev})	Visually defined in GIS, verified with geotagged photos. Does not include terraces and other non-accessible valley-bottom areas	2013 DEM, NYCDEP field data
Channel width (W_c)	Width of channel, June 2018	Field data
Number of channels (#ch)	Average number of channels per reach, derived from number of channels present during cross-sectional surveys	Field data
Wood volume (LW)	Length*width*height of mapped wood	Field data
Jam proportion (LW_J)	Volume of wood within jams/total volume of wood per reach	Field data
Constriction ratio	Effective valley width/effective valley width upstream	GIS 10.5.1
Backwater ratio	Effective valley width/effective valley width downstream	GIS 10.5.1
Sinuosity	Length of channel/straight line distance along valley	GIS 10.5.1
Valley confinement (C_v)	Length of channel abutting valley wall/total length of channel	Fryirs *et al*. (2016)
Valley bottom confinement (C_{VB})	Length of channel abutting valley floor confinement/total length of channel	Fryirs *et al*. (2016)

inputs from adjacent hillslopes. Table 2 lists variables derived from the field measurements and used in analyses for subreaches within reach A4.

DEM analyses

Two hydro-flattened DEMs with 1 m horizontal resolution were available to support this investigation (RACNE, 2012; Dewberry, 2015). Each DEM was developed from airborne LiDAR flown over portions of the Catskill Mountains in 2009 and 2013–14 ('2014'), allowing us to evaluate geomorphic adjustment in the river corridor during the period that included the August 2011 flood using geomorphic change detection methods in a GIS platform (Wheaton *et al*., 2010). DEM processing included application of a bare-earth process using algorithms to remove all vegetation and structures. The LiDAR method could not get data for the earth surface below water surfaces, introducing uncertainty associated with channel depth below the stream stage elevation for each time period. Base flow conditions, which are shallow in this small stream, are assumed for each DEM. The 2009 DEM was derived from extensively ground-truthed airborne LiDAR data collected in April 2009 as part of the New York State Digital Ortho Program under contract with New York City Department of Environmental Protection (RACNE, 2012). The 2014 DEM was developed for the US Geological Survey from airborne LiDAR flown from November 2013 to June 2014 over three counties in New York State. The resulting bare-earth DEM encompasses the entirety of the study area. Average point density for the entire Catskill region for both DEMs met the 1 m horizontal accuracy standard at the 95% confidence level. The 2009 DEM consolidated vertical accuracy (CVA) of 0.36 m at the 95% confidence level was required for FEMA floodplain mapping specifications. The 2009 DEM averages point spacing at 0.945 m and the 2014 DEM averages 1 point per 0.7 m^2. The reported CVA for the 2014 DEM met the project criteria of 0.26 m at the 95% confidence level. [The CVA is the assessment of vertical accuracy that composites the different accuracies associated with the all-terrain conditions, not just the assumed open-terrain land cover category, which is assessed by a fundamental vertical accuracy (FVA) metric.]

A visual inspection of each DEM detected more 'noise' in the 2014 DEM, especially in upland forested terrain. DEM differencing included a limit of detection of 0.25 m to account for unexplained noise, potential impacts of stream stage, and differences in vertical accuracy between the two DEMs. Given the lack of a more detailed accounting of uncertainty within and between the two DEMs, this analysis focuses on identifying clear degradation and aggradation zones, their longitudinal relationships, and relative magnitudes. To this end, we used the average of the grid cells within the bounds of the active channel in a differenced DEM to calculate the reach-averaged change in channel-bed elevation.

Hydraulic modelling

To provide additional insight into the longitudinal distribution of hydraulic force, the potential for sediment transport, and the hydraulic effects of large wood in reach A4, we used the one-dimensional (1D) steady-flow HEC-RAS hydraulic model (Brunner, 2016) to route three discharges through channel geometry derived from the 2014 DEM and field-surveyed cross-sections. We modelled a 1-year flow (Q = 4.5 m^3 s^{-1}), a 5-year flow (Q = 15.4 m^3 s^{-1}), and the estimated discharge of the 2011 flood (Q = 42.5 m^3 s^{-1}) based on the gauge downstream from the study reach. The 5-year flow occurred during the study and we flagged high-water marks shortly after the flood, which helped to calibrate roughness and other

© 2020 John Wiley & Sons, Ltd.

coefficients used in modelling. We modelled mixed critical and supercritical flow with a normal depth boundary condition and held Manning *n* values (0.03 within the bankfull channel and 0.04 for overbank areas) constant. We used 36 field-measured cross-sections, with cross-sections interpolated every 1 m to connect surveyed cross-sectional geometries, resulting in 710 modelled cross-sections over a channel length of 690 m. For each discharge, we modelled two scenarios: one that included surveyed large wood and one with the wood removed (Hinshaw, 2019). We altered 21 of the 36 surveyed cross-sections to remove large wood. We also modelled the same three discharges through the entire study reach using 159 DEM-derived cross-sections with no wood removal.

Statistical analyses

Our hypothesis has multiple components. For the portion proposing that changes in channel-bed elevation correlate with wood load, we used linear regressions to evaluate the relationships within the subreaches of A4 and for all alluvial reaches. We used Wilcoxon pairwise comparisons to evaluate differences between bedrock and alluvial reach geometry and net erosion during 2009–14. For the portion of the hypothesis proposing that grain-size characteristics correlate with wood load, we used two sets of analyses. For these analyses, we concentrated on reach A4 because of the detailed channel geometry and bed substrate data from this reach.

For the first set of analyses involving wood load and grain-size characteristics, all wood, valley geometry, and sediment variables for A4 were used in the `cor()` function in R statistical software. This function calculates Pearson correlation statistics for each variable as a singular predictor of and response to every other variable in the dataset. The output was trimmed in order to examine only the response of sediment distribution attributes to wood and valley geometry variables. Correlations were compared and the most suitable variables with the highest correlations were selected for inclusion in a multiple linear regression. We selected the median grain size (D_{50}) to represent grain size and the gradation coefficient (σ_g) to represent variability and sorting within the sediment distribution.

We selected eight variables for significance testing of the Pearson correlation statistic. Seven of the nine variables in bold font in Table 2 were tested directly. The ratio of effective valley width to geologic valley width was used to represent the active proportion of the valley floor. These eight variables relate to valley geometry or wood and either show a high Pearson correlation value or are qualitatively inferred to be an important influence on geomorphic processes. The eight variables were analysed for significance of correlation with the `cor.test()` function in R using a 90% confidence level.

For the second set of analyses involving wood load and grain-size characteristics, we used multiple linear regressions to evaluate potential predictor variables of D_{50} and σ_g in the subreaches of A4. The selection criteria for input variables were based on correlation strengths using the Akaike information criterion corrected for small sample sizes (AICc) (Hurvich and Tsai, 1989). The small sample size (n =8) and the probability that the six selected predictor variables used for multiple linear regression analysis are collinear yielded a qualitative assessment of which predictor variables most strongly influence bed substrate.

For the portion of the hypothesis that wood load correlates inversely with modelled velocity, we used a series of Welch two-sample *t*-tests with a 95% confidence interval to evaluate statistical differences in velocity associated with changes in valley geometry or the presence of wood. These tests were completed with the `t.test()` function in R. We statistically analysed model results from the field-surveyed and interpolated cross-sections (rather than just the surveyed cross-sections) because the more inclusive dataset had the lowest average deviation (0.15 m) from the observed water-surface elevations for the 5-year flow. Calibration to force HEC-RAS to match precisely the observed water-surface elevations is inappropriate because of the porosity of logjams. Porosity allows some water to flow through a logjam, whereas we represented jams as impermeable blockages in the modelled channel geometry. We expect the modelled water surfaces to deviate slightly from actual high-water marks as a result of enhanced modelled backwater effect and a constant Manning's n. We compared reach-averaged velocity with and without the presence of large wood.

Limitations

Our ability to test our hypothesis is limited by at least three factors. First, we are inferring geomorphic effects of the 2011 flood using changes in channel geometry based on 2009 and 2014 LiDAR and field measurements in 2018, rather than direct measurements immediately pre- and post-flood. As part of this approach, we assume that surveyed logjams were present or formed during Hurricane Irene. Our analyses thus include changes over a period of years, although the 5-year flow that occurred during this study did not produce notable changes in channel morphology (e.g. no changes in the longitudinal locations of alluvial and bedrock reaches). Second, the dynamics of large wood and sediment likely influenced each other during and after the flood, whereas we are treating large wood as an effectively static feature and evaluating velocity and substrate characteristics in the vicinity of the wood. It is not feasible to directly measure interactions during a flood of this magnitude in a field setting, so the inferences developed based on correlations present after the flood represent the most realistic field-based approach to the questions we examine in this paper. Third, use of the 1D HEC-RAS model to evaluate the hydraulic effects of logjams is based on a highly simplified scenario in which a logjam is approximated by a geometric block protruding from the channel bed. This approximation does not incorporate the porosity of a logjam or the potential for breakage or movement of individual pieces within the jam or the entire jam during high discharges. As the ability to represent complex, porous three-dimensional (3D) structures such as logjams (Spreitzer *et al.*, 2020a,b) in numerical hydraulic modelling improves, it will likely become more feasible to simulate the effects of numerous individual logjams along a channel, but we believe that the model-based inferences reported here represent a reasonable first approximation of the effects of wood over a study area that is 3 km long.

Results

Hydraulic modelling

Comparison of field-marked and modelled water-surface elevations for the 5-year flow indicated less than ±0.5% difference in elevation (see Table S1 in the online Supporting Information), suggesting that the parameterization used in the HEC-RAS runs reasonably approximates flow conditions. We used HEC-RAS modelled values of shear stress in subreaches of reach A4 to assess potential bed-material mobility (see Table S2 in the online Supporting Information). Based on the relation for

© 2020 John Wiley & Sons, Ltd.

entrainment from a gravel bed of mixed grain sizes from Komar (1987), average shear stress during the 5-year and 2011 flood flows greatly exceeds critical shear stress for the D_{50} of the bed surface. This suggests that the bed surface can be mobilized at these flows and that spatial characteristics of bed substrate can reflect local influences such as accumulations of large wood.

Bedrock versus alluvial reaches

Pairwise comparisons of bedrock and alluvial reaches indicate the following: Bedrock and alluvial reaches do not differ significantly with respect to reach length (p = 0.4) or gradient (p = 0.38), although alluvial reaches tend to be longer (median 180 m for alluvial, 104 m for bedrock). Area of landslides associated with bedrock and alluvial reaches also does not differ significantly (p = 0.23), suggesting that the location of alluvial reaches does not directly reflect the presence of hillslope sediment inputs. Alluvial reaches have a significantly greater active channel width (p = 0.08). Reach-averaged velocity does not differ significantly between bedrock and alluvial for the modelled 1-year (p = 0.14) and 5-year (p =0.10) flows but is significantly lower in alluvial reaches (p =0.06) for the modelled 2011 flow. The 2009–14 elevation change did not differ significantly between bedrock and alluvial reaches (p = 0.49). Similarly, the 2009–14 volume change did not differ significantly between bedrock and alluvial reaches (p = 0.89). The population of bedrock reaches did have slightly greater average incision during this period (−0.32 m for bedrock, −0.10 m for alluvial reaches), but this change is close to or within the 0.25 m detection limit for the DEM differencing. Given the much higher erosional resistance of bedrock reaches, the fact that net change during the 2011 flood was comparable between bedrock and alluvial reaches suggests substantial sediment transport and erosion of bedrock during the flood. The bedrock reaches in which highly fractured mudstone was exposed were likely most susceptible to erosion.

Correlations between wood and substrate characteristics within reach A4

We hypothesized that greater wood loads, by causing more flow obstruction and hydraulic roughness, would correspond to reduced bedload transport capacity and finer bed grain sizes. Tests using two measures of channel substrate, D_{50} and σ_g, for correlations with singular predictor variables related to valley geometry and wood load indicate that four predictor variables correlate significantly with D_{50} and σ_g within reach A4. Significant predictor variables are proportion of total wood load in jams, number of channels, channel gradient, and proportion of clast counts recorded as bedrock (Table 3). Greater proportion of wood in jams and greater number of active channels correlate with finer grain size and smaller sediment gradation, whereas steeper channel gradient and greater proportion of exposed bedrock correlate with larger grain size and larger gradation. The absence of a significant correlation between grain size and wood volume (rather than proportion of wood in jams) suggests that wood has a much greater influence on sediment dynamics when the wood is part of a jam.

Multiple linear regression to qualitatively assess the strength of combined wood and valley geometry variables to predict D_{50} results in selection of six predictor variables: gradient, bedrock proportion, active valley proportion, number of channels, jam proportion, and wood volume [Equation 1)]. Equation 1 produces a statistically significant prediction of D_{50} (adjusted R^2 =0.996 and p = 0.046) but is intended for conceptual use

Table 3. Pearson coefficients of determination for correlations with D_{50} and σ_g; bold values are significant

	D_{50}	Direction of correlation	Significance at 90% confidence level	σ_g	Direction of correlation	Significance at 90% confidence level
Jam proportion	**0.69**	–	p = 0.01	**0.53**	–	p = 0.041
Active proportion of valley floor	0.35	–	p = 0.12	0.40	–	p = 0.09
Number of channels	**0.76**	–	p = 0.0045	**0.51**	–	p = 0.045
Channel gradient	**0.45**	+	p = 0.067	**0.48**	+	p = 0.058
Bedrock proportion	**0.74**	+	p = 0.0064	**0.40**	+	p = 0.0000075

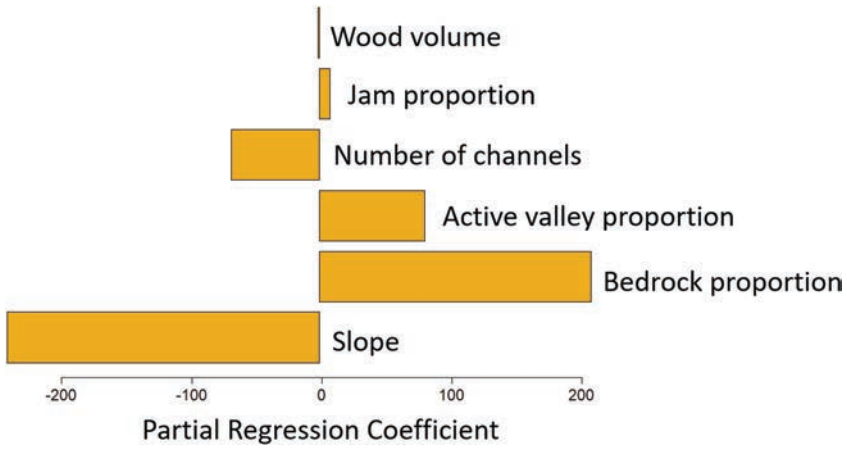

FIGURE 3. Partial regression coefficient estimations for median grain size, represented in a bar graph to show relative influence of each variable. The variables are stacked in order of significance. [Colour figure can be viewed at wileyonlinelibrary.com]

© 2020 John Wiley & Sons, Ltd.

only because of the small sample size when including only A4 subreaches:

$$D_{50}=128.6–239.8(S)+209.1(Br)+80.9(W_{ev})–68(\#ch)+8.15(LW_J)–0.24(LW) \quad (1)$$

(Abbreviations defined in Table 2.) Among the six predictor variables, channel gradient (S) and the proportion of bedrock (Br) are by far the strongest predictors (Figure 3). Higher channel gradient and greater proportion of bedrock exposed in the channel correspond to larger D_{50}. Multiple linear regression for σ_g did not produce a significant model (p = 0.1416), although the results suggest that channel gradient is again the strongest influence on sediment gradation.

Differences in elevation from 2009 to 2014 (Figure 4) indicate the location of predominantly erosional and depositional zones within subreaches of A4. Subreaches A4a and A4b, which are underlain primarily by mudstone, eroded. Most of the remainder of A4 aggraded, with the largest aggradation in A4d and A4e. Particle size distributions in individual subreaches gradually fine downstream from A4a to A4e and then coarsen downstream from A4e (Figure 5).

Correlations between wood and channel change in the study area

Simple bar graphs of wood load and elevational change in downstream order for the entire study area indicate that wood is predominantly stored in reach A4 (Figure 6). The segments with greatest channel erosion are immediately upstream from and within the upper portion of reach A4, whereas those with the greatest aggradation are in the middle of reach A4. Examining volume change during 2009–14 in relation to wood, there is a significant difference (p = 0.074) between reaches with wood (mean volume change 329 m^3) and reaches without wood (mean volume change −751 m^3). Wood load does not correlate with channel-bed elevational change during 2009–

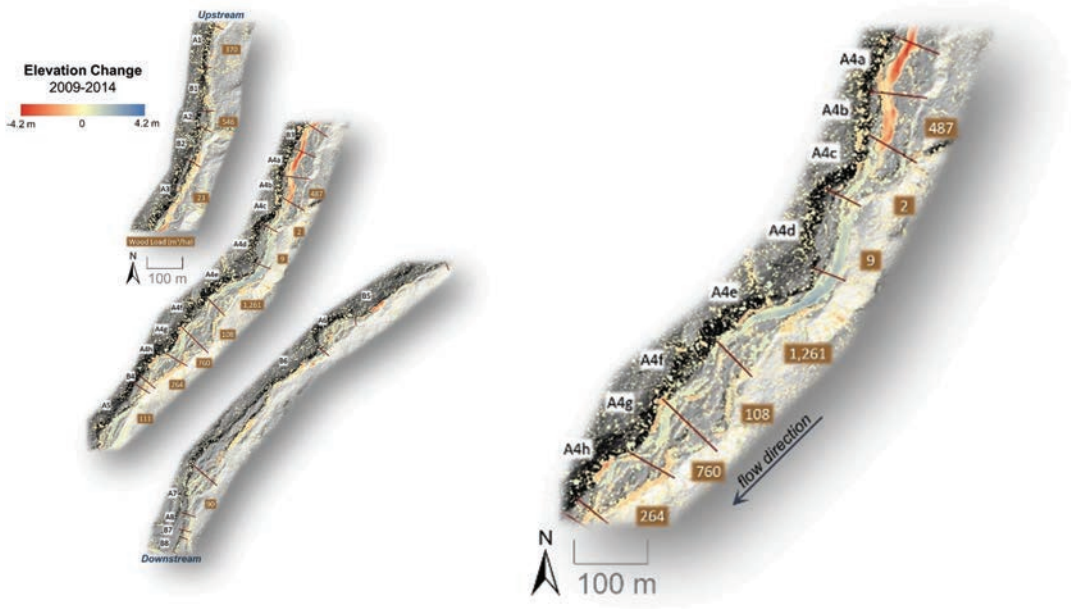

FIGURE 4. Map of difference in elevation between 2009 and 2014. (A) The entire study area. Reach identifiers are at left for each reach and wood load (m^3 ha^{-1}) is at right. The elevation change scale is symmetrical about 0, but the maximum aggradation was 2.8 m and the maximum erosion was 4.3 m. (B) The map clipped to the A4 reach. [Colour figure can be viewed at wileyonlinelibrary.com]

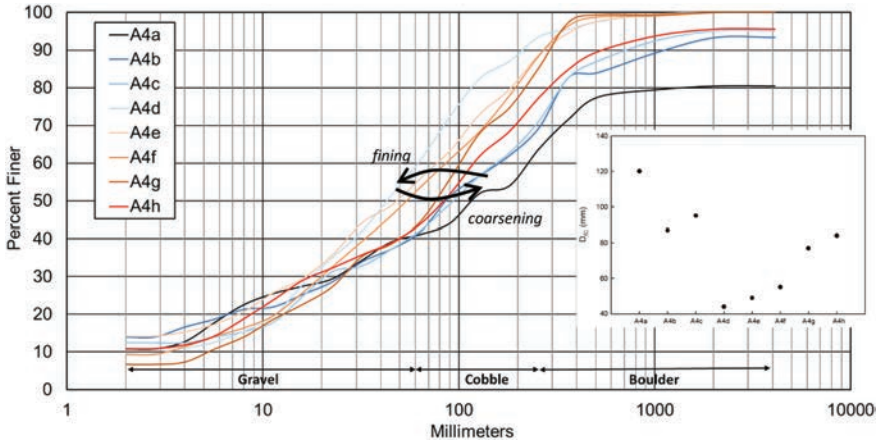

FIGURE 5. Particle size distributions in the A4 reach. The curved arrows highlight the fining pattern from A4a to A4e and coarsening from A4e to A4h. The inset plot shows the D_{50} values for each subreach. [Colour figure can be viewed at wileyonlinelibrary.com]

© 2020 John Wiley & Sons, Ltd.

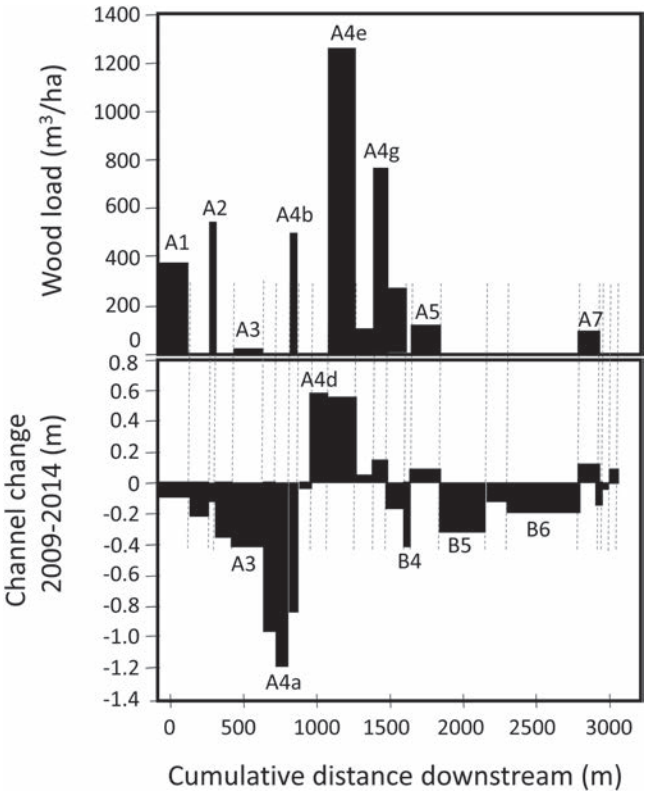

FIGURE 6. Bar graph illustrating longitudinal variation in wood load (upper plot) and change in channel-bed elevation between 2009 and 2014 (lower plot) for all reaches and subreaches in the study area. Selected reaches are identified in each plot to facilitate interpretation.

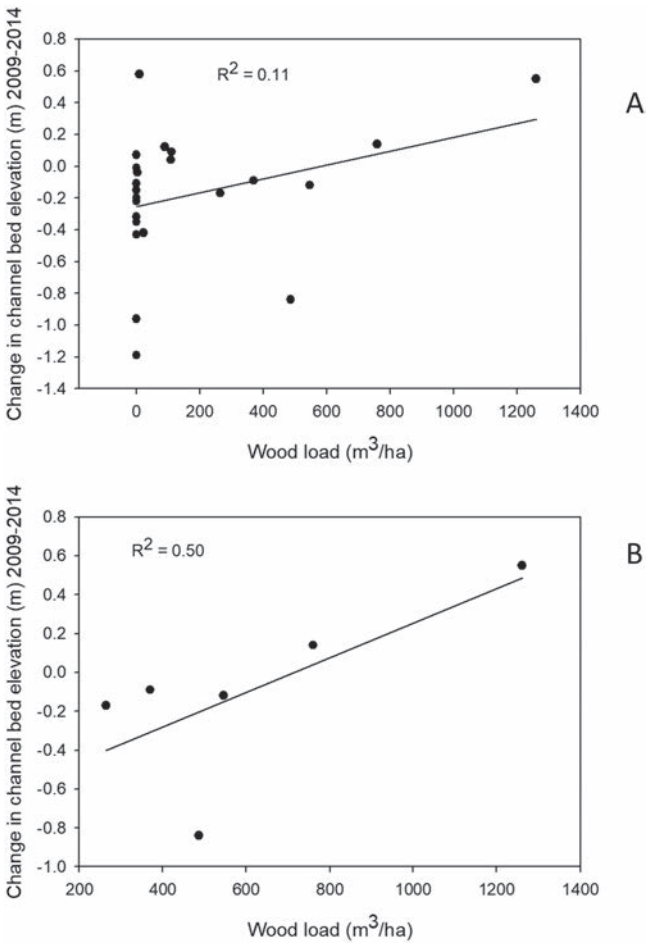

FIGURE 7. (A) Wood load versus 2009–14 change in channel-bed elevation for all reaches and subreaches. (B) Wood load versus channel change for only reaches and subreaches with wood load ≥ 200 m^3 ha^{-1}. Outlier near the bottom of the plot is subreach A4b.

14 when all reaches are included, but there is a significant correlation (R^2 = 0.56, p = 4.23e-5) between wood load and net volume of sediment eroded or aggraded (Figure 7A). The data in Figure 7A suggest a potential threshold relationship between wood load and channel change. When reaches with wood loads less than 200 m^3 ha^{-1} are removed from consideration, greater wood loads do correlate with channel-bed aggradation (Figure 7B).

In addition to these interpretations of statistical analyses, we see evidence of an aggradational bulge within reach A4. The active channel is notably poorly defined in subreach A4e and bed gradient steepens partway down the reach (Figure 8), which suggests an aggradational wedge. The greatest net erosion in an alluvial reach during the 2009–14 period is in A4a and A4b and the greatest net aggradation is in A4d and A4e (Figure 6). A4e also has by far the highest wood load (Table 1). These longitudinal trends in wood and channel change (Figure 4), as well as substrate characteristics (Figure 5), suggest that an aggradational bulge is currently located at A4e. Although we found no significant difference in mapped landslide area between bedrock and alluvial reaches, it is worth noting that 60% of the mapped landslides occur within alluvial reaches and all of the largest landslides occur within A4. However, within-channel erosion of upstream reaches likely contributed more of the sediment currently stored in A4 than did landslides: a generalized estimate of cumulative erosion from reach A1 through reach A4c suggests four times as much sediment mobilized from the valley bottom as from landslides. Field observations suggest that substantial wood was recruited to A4e during the 2011 flood and this wood might be enhancing the formation of what investigations elsewhere refer to as a hot spot of sediment storage (Rigon *et al.*, 2012; Czuba and Foufoula-Georgiou, 2015). Some of the large wood pieces with complex shapes in A4e appear to have come from nearby landslides, but many pieces show evidence of downstream transport to A4e.

We do not know whether the aggradation at A4e represents a slowly moving wave that will translate or disperse to downstream alluvial reaches with time. The concentration of large landslides within reach A4 suggests that the current position of the aggradational bulge is at least partly influenced by local introduction of sediment, but the evidence of substantial incision upstream, along with transport of wood and sediment downstream to A4, suggests that the bulge did not result solely from local sediment sources. The exceptionally large wood load within A4e is likely to influence downstream movement of the aggradational bulge and result in dispersion of the sediment wave.

Effects of large wood on reach-averaged velocity

We hypothesized that the greater flow obstruction and hydraulic roughness associated with the presence of logjams would correspond to lower modelled values of reach-averaged velocity. Results from HEC-RAS modelling suggest that the presence of large wood does not create statistically significant differences in velocity averaged over the A4 subreach at lower flows (1 and 5-year return interval). Wood does significantly (p = 0.002612) reduce A4 reach-average velocity during floods of the magnitude that occurred in 2011.

© 2020 John Wiley & Sons, Ltd.

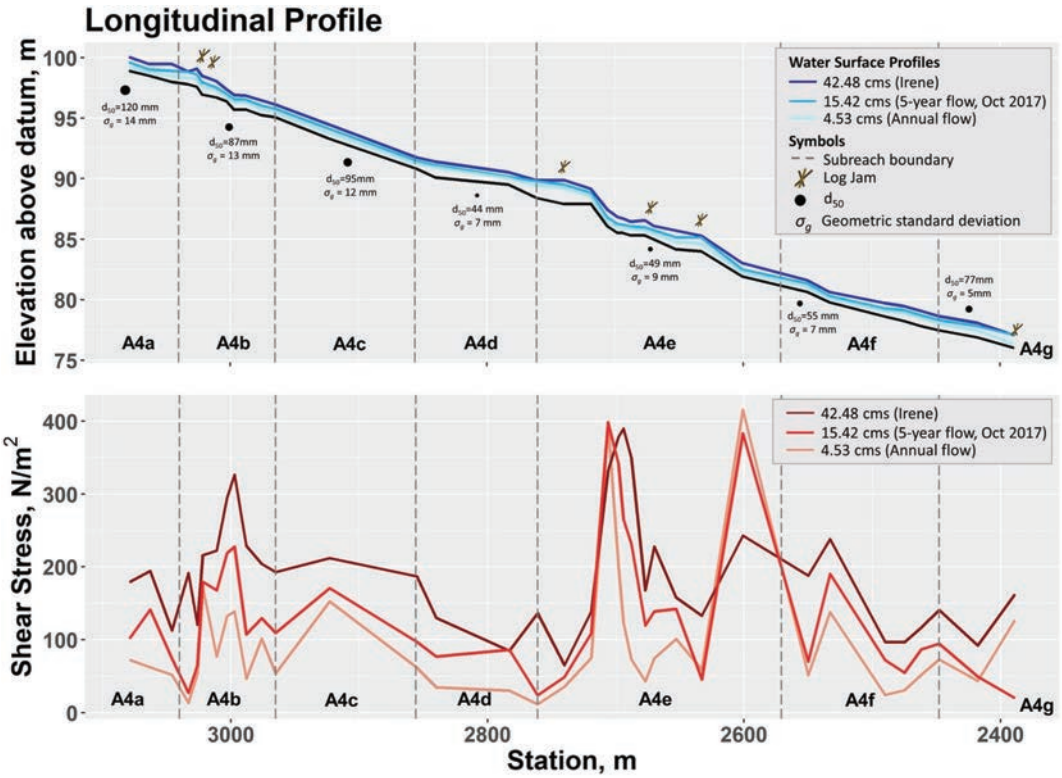

FIGURE 8. Longitudinal profile of A4 reach with grain size per subreach shown in upper plot. Black line represents the channel bed; blue lines are the water surface modelled with wood for three discharges. Black circles represent D_{50} of grain size within each subreach, with value (mm) and standard deviation listed below each circle. Log jams are shown by brown symbols. The six jams shown were chosen for proximity analysis of velocities within 20 m upstream of the jams. Longitudinal variation in cross-sectionally averaged, modelled shear stress for the three discharges shown in lower plot. [Colour figure can be viewed at wileyonlinelibrary.com]

Discussion

We hypothesized that, within alluvial reaches, geomorphic response to the flood would correlate with wood load. The results indicate that channel changes through time in relation to wood load are more nuanced than we originally expected. At the inter-reach scale, abundance of wood does not correlate significantly with channel elevational change or with modelled reach-average velocity for the annual peak flow or 5-year flow. However, the model results suggest that wood does significantly reduce reach-scale average velocity during higher discharges, such as the 2011 flood. Within reach A4, a greater proportion of wood in jams corresponds to smaller values of D_{50} and σ_g at the subreach scale. These results suggest that individual logjams can locally influence sediment dynamics (e.g. Keller and Swanson, 1979; Lisle, 1995; Abbe and Montgomery, 1996; Comiti *et al.*, 2008) and channel response to flooding (Brummer *et al.*, 2006; Sear *et al.*, 2010; Dixon *et al.*, 2016). Censoring the inter-reach data to remove reaches with wood loads less than 200 m^3 ha^{-1} also reveals a significant inter-reach influence from wood, suggesting that a threshold wood load is necessary before reach-scale wood influences occur.

We are not aware of any other studies that have searched for or discussed potential thresholds in wood-related effects on erosion or sedimentation, although this has been identified as a knowledge gap for understanding large wood in streams (Wohl, 2017). In this context, it is useful to note that wood load within the alluvial reaches of Biscuit Brook is comparable to wood loads reported for similar drainage areas in unmanaged watersheds around the world (Figure 9). Also, the stability of wood pieces and jams varies among reaches. In the upstream portions of Biscuit Brook, large wood pieces are commonly ramps or bridges with one or both ends, respectively, on the valley margins above fluvial processes. Wood pieces also tend to include complex, relatively delicate branches and rootwads, suggesting limited downstream transport of the wood (see Figure S2 in the online Supporting Information). Mobility of wood appears to increase with distance downstream within A4 and in reaches downstream of A4, as evidenced by simpler pieces that are aligned perpendicular to flow in logjams, commonly around the base of live trees.

Analyses of wood load, modelled velocity, and bed grain-size data thus suggest that, especially at the higher discharges competent to move the cobble and boulder substrate present in Biscuit Brook, concentrations of large wood in the form of jams can significantly reduce reach-average velocity, resulting in finer bed sediment than is present in channel reaches with less wood. As noted earlier, the proportion of wood in jams correlates more strongly with median bed grain size and gradation coefficient than does wood load, suggesting that wood in jams more strongly influences grain-size characteristics than do dispersed pieces. As total wood load increases, the trapping efficiency for wood entering the reach is likely to increase (Beckman and Wohl, 2014b; Davidson *et al.*, 2015), which may help to explain the inferred threshold relationship between wood load and channel-bed aggradation (Figure 7B): greater wood load equates to greater proportion of wood in jams and more bed aggradation and bed fining.

The presence of large wood in the alluvial reaches of Biscuit Brook may also contribute to channel resilience to large floods. As noted earlier, reach-averaged bed elevation changes in alluvial versus bedrock reaches during 2009–14 were not significantly different. The 2011 flood was competent to mobilize bed material throughout the reach, and visual observations of recent erosional and depositional features throughout the

© 2020 John Wiley & Sons, Ltd.

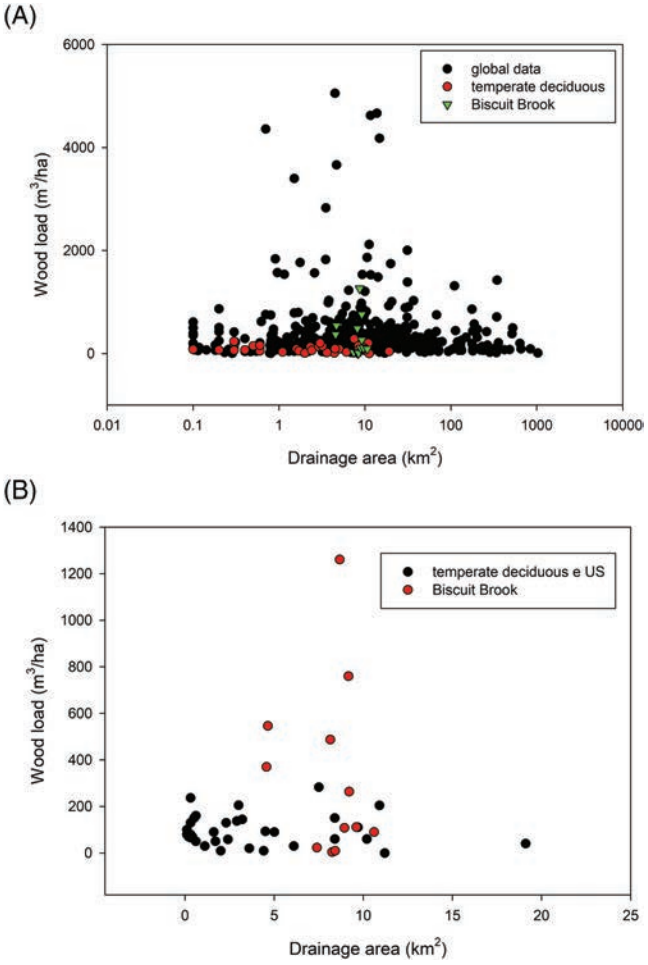

FIGURE 9. (A) Wood load versus drainage area for a global dataset of old-growth or unmanaged forest. (B) Wood load versus drainage area for old-growth or unmanaged forests in the eastern United States. [Colour figure can be viewed at wileyonlinelibrary.com]

study reach during field work suggest extensive bed mobilization during the flood. The net erosion of relatively resistant bedrock reaches during 2009–14 also suggests erosion during the flood. The presence of very little net change in bed elevation within alluvial reaches during 2009–14 (average −0.10m, which is below the uncertainty limit) and the net aggradation in subreaches A4d and A4e, which corresponds to high wood load in A4e, suggests that large wood reduced net erosion within alluvial reaches during 2009–14. The significant positive correlation between wood load and net aggradation, and the significant difference between volume of aggradation in reaches with and without wood, support this idea. Given the importance of large wood and alluvial substrate in providing river ecosystem services such as hyporheic exchange (Sawyer *et al.*, 2011), particulate organic matter storage (Beckman and Wohl, 2014a; Livers and Wohl, 2016), and habitat abundance and diversity (e.g. Richmond and Fausch, 1995), we infer that the presence of large wood during and after the 2011 flood enhanced the resilience of Biscuit Brook to this flood.

Future work that improves the ability to characterize logjam shape and permeability (e.g. Spreitzer *et al.*, 2020b) and to numerically model the effects of multiple logjams on hydraulics could greatly enhance the ability to quantify how wood distribution influences geomorphic processes during a range of flow magnitudes. Ideally, pre- and post-flood data could be used to examine the relative importance of differing wood loads and spatial distribution of wood on hydraulics, sediment dynamics, and channel response to floods, although pre-flood data are rare for large, unpredictable floods such as the 2011 flooding in Biscuit Brook. The threshold relationship that we infer between large wood load and channel change is specific to this field site, but studies focusing on analogous potential thresholds at different sites would be very useful in testing this inference and in potentially creating guidelines for wood restoration targets as part of river management.

Conclusions

Previous studies suggest that abundant large wood, whether in the form of dispersed pieces or logjams, can strongly influence the longitudinal distribution of bedrock and alluvial segments in coarse-grained mountain streams (e.g. Montgomery *et al.*, 1996) and whether a channel reach is predominantly a sediment source or a sediment sink in lowland sand-bed channels (e.g. Brooks *et al.*, 2003). At Biscuit Brook, stronger correlations between valley geometry and grain size than between abundance of wood and grain size at the reach- to subreach-scale likely reflect the pronounced downstream variations in valley geometry that are associated with longitudinal differences in bedrock lithology. Wood within alluvial reaches along Biscuit Brook correlates significantly with a finer bed grain size and smaller gradation of bed sediment. Above a threshold wood load value of 200 m^3 ha^{-1}, wood load also correlates with change in reach-averaged channel-bed elevation during the period including the 2011 flood. The presence of an aggradational bulge partway down Biscuit Brook, which corresponds to high wood loads, does not appear to be solely created by the wood, although the wood likely influences the persistence of this bulge.

We conclude that the degree to which large wood influences sediment dynamics and channel response to flooding depends strongly on the characteristics of a channel and valley and the relative quantities of large wood and sediment within the channel. Because the effects of wood may be greatest above a threshold wood load and when wood is concentrated in jams, restoring only isolated pieces or a single jam to a channel that once had a much larger wood load is likely to create only limited, local geomorphic effects (e.g. Brooks *et al.*, 2004; Roni *et al.*, 2015).

Acknowledgements—We thank Mark Vian (New York City Department of Environmental Protection) and Karen Rauter (Rondout-Neversink Stream Management Program) for initiating and funding this project. We thank Cassidy Ryan, Douglas Thompson, Anna Marshall, Emma Brooks, Clare Loughlin, Emily Polinsky, and the Ulster County Community College Watershed Conservation Corps for assistance with field work, and Sara Rathburn and Ryan Morrison for useful reviews of an earlier version of this document. The manuscript benefited from comments by two anonymous reviewers.

Conflict of Interest

The authors declare no conflict of interest.

Data Availability Statement

The basic data used in the analyses are presented in the online Supporting Information.

© 2020 John Wiley & Sons, Ltd.

References

Abbe TB, Montgomery DR. 1996. Large woody debris jams, channel hydraulics and habitat formation in large rivers. *Regulated Rivers: Research & Management* **12**: 201–221.

Beckman ND, Wohl E. 2014a. Carbon storage in mountainous headwater streams: the role of old-growth forest and logjams. *Water Resources Research* **50**: 2376–2393.

Beckman ND, Wohl E. 2014b. Effects of forest stand age on the characteristics of logjams in mountainous forest streams. *Earth Surface Processes and Landforms* **39**: 1421–1431.

Bellmore JR, Baxter CV. 2014. Effects of geomorphic process domains on river ecosystems: a comparison of floodplain and confined valley segments. *River Research and Applications* **30**: 617–630.

Brooks AP, Brierley GJ, Millar RG. 2003. The long-term control of vegetation and woody debris on channel and flood-plain evolution: insights from a paired catchment study in Australia. *Geomorphology* **51**: 7–29.

Brooks AP, Gehrke PC, Jansen JD, Abbe TB. 2004. Experimental reintroduction of woody debris on the Williams River, NSW: geomorphic and ecological responses. *River Research and Applications* **20**: 513–536.

Brummer CJ, Abbe TB, Sampson JR, Montgomery DR. 2006. Influence of vertical channel change associated with wood accumulations on delineating channel migration zones, Washington, USA. *Geomorphology* **80**: 295–309.

Brunner G. 2016. *HEC-RAS River Analysis System*. Hydraulic Reference Manual, vol. 5. US Army Corps of Engineers, Hydrologic Engineering Center: Davis, CA.

Buffington JM, Montgomery DR. 1999. Effects of hydraulic roughness on surface textures of gravel-bed rivers. *Water Resources Research* **35**: 3507–3521.

Collins BD, Montgomery DR, Fetherston KL, Abbe TB. 2012. The floodplain large-wood cycle hypothesis: a mechanism for the physical and biotic structuring of temperate forested alluvial valleys in the North Pacific coastal ecoregion. *Geomorphology* **139–140**: 460–470.

Comiti F, Andreoli A, Mao L, Lenzi MA. 2008. Wood storage in three mountain streams of the southern Andes and its hydro-morphological effects. *Earth Surface Processes and Landforms* **33**: 244–262.

Comiti F, Lucia A, Rickenmann D. 2016. Large wood recruitment and transport during large floods: a review. *Geomorphology* **269**: 23–39.

Czuba JA, Foufoula-Georgiou E. 2015. Dynamic connectivity in a fluvial network for identifying hotspots of geomorphic change. *Water Resources Research* **51**: 1401–1421.

Davidson SL, MacKenzie LG, Eaton BC. 2015. Large wood transport and jam formation in a series of flume experiments. *Water Resources Research* **51**: 10065–10077.

Dethier E, Magilligan FJ, Renshaw CE, Nislow KH. 2016. The role of chronic and episodic disturbances on channel-hillslope coupling: the persistence and legacy of extreme floods. *Earth Surface Processes and Landforms* **41**: 1437–1447.

Dewberry. 2015. *Ulster, Duchess, and Orange Counties, New York – Sandy LIDAR*. U.S. Geological Survey: Rolla, MO.

Dixon SJ, Sear DA, Odoni NA, Sykes T, Lane SN. 2016. The effects of river restoration on catchment scale flood risk and flood hydrology. *Earth Surface Processes and Landforms* **41**: 997–1008.

Gippel CJ. 1995. Environmental hydraulics of large woody debris in streams and rivers. *Journal of Environmental Engineering* **121**: 388–395.

Hauer FR, Locke H, Dreitz VJ, Hebblewhite M, Lowe WH, Muhlfeld CC, Nelson CR, Proctor MF, Rood SB. 2016. Gravel-bed river floodplains are the ecological nexus of glaciated mountain landscapes. *Science Advances* **2**: e1600026.

Hinshaw SK. 2019. Relative influences of valley geometry and wood on sediment distribution in Biscuit Brook, NY. MS thesis, Colorado State University, Fort Collins, CO.

Hurvich CM, Tsai C. 1989. Regression and time series model selection in small samples. *Biometrika* **76**: 297–307.

Johnson SL, Swanson FJ, Grant GE, Wondzell SM. 2000. Riparian forest disturbances by a mountain flood – the influence of floated wood. *Hydrological Processes* **14**: 3031–3050.

Julien, PY. 2010. *Erosion and Sedimentation, 2nd ed*. Cambridge, UK: Cambridge University Press.

Keller EA, Swanson FJ. 1979. Effects of large organic material on channel form and fluvial process. *Earth Surface Processes* **4**: 361–380.

Komar PD. 1987. Selective grain entrainment by a current from a bed of mixed sizes; a reanalysis. *Journal of Sedimentary Research* **57**: 203–211.

Lisle TE. 1995. Effects of coarse woody debris and its removal on a channel affected by the 1980 eruption of Mount St. Helens, Washington. *Water Resources Research* **31**: 1797–1180.

Livers B, Wohl E. 2016. Sources and interpretation of channel complexity in forested subalpine streams of the Southern Rocky Mountains. *Water Resources Research* **52**: 3910–3929.

Magilligan FJ, Buraas EM, Renshaw CE. 2015. The efficacy of stream power and flow duration on geomorphic responses to catastrophic flooding. *Geomorphology* **228**: 175–188.

Manners RB, Doyle MW, Small MJ. 2007. Structure and hydraulics of natural woody debris jams. *Water Resources Research* **43**: W06432.

Marcus WA, Marston RA, Colvard CR, Gray RD. 2002. Mapping the spatial and temporal distributions of woody debris in streams of the Greater Yellowstone Ecosystem, USA. *Geomorphology* **44**: 323–335.

Montgomery DR, Abbe TB, Peterson NP, Buffington JM, Schmidt KM, Stock JD. 1996. Distribution of bedrock and alluvial channels in forested mountain drainage basins. *Nature* **381**: 587–589.

Pontyondy, J & Bunte, K. 2002. Analyzing pebble count data collected by size classes. *Version 1.0a. Excel Spreadsheet*. Fort Collins, Colorado: USDA Forest Service, Rocky Mountain Research Station.

RACNE. 2012. Terrain Surface Standards, project report, CAT-393 Airborne Lidar Quality Assurance and GIS Terrain Data Development, Phase 2, New York City Department of Environmental Protection.

Richmond AD, Fausch KD. 1995. Characteristics and function of large woody debris in subalpine Rocky Mountain streams in northern Colorado. *Canadian Journal of Fisheries and Aquatic Sciences* **52**: 1789–1802.

Righini M, Surian N, Wohl E, Marchi L, Comiti F, Amponsah W, Borga M. 2017. Geomorphic response to an extreme flood in two Mediterranean rivers (northeastern Sardinia, Italy): analysis of controlling factors. *Geomorphology* **290**: 184–199.

Rigon E, Comiti F, Lenzi MA. 2012. Large wood storage in streams of the eastern Italian Alps and the relevance of hillslope processes. *Water Resources Research* **48**: W01418. https://doi.org/10.1029/2010WR009854

Roni P, Beechie T, Pess G, Hanson K. 2015. Wood placement in river restoration: fact, fiction, and future direction. *Canadian Journal of Fisheries and Aquatic Sciences* **72**: 466–478.

Ruiz-Villanueva V, Badoux A, Rickenmann D, Bockli M, Schlafli S, Steeb N, Stoffel M, Rickli C. 2018. Impacts of a large flood along a mountain river basin: the importance of channel widening and estimating the large wood budget in the upper Emme River (Switzerland). *Earth Surface Dynamics* **6**: 1115–1137.

Sawyer AH, Cardenas MB. 2012. Effect of experimental wood addition on hyporheic exchange and thermal dynamics in a losing meadow stream. *Water Resources Research* **48**: W10537.

Sawyer AH, Cardenas MB, Buttles J. 2011. Hyporheic exchange due to channel-spanning logs. *Water Resources Research* **47**: W08502.

Sear DA, Millington CE, Kitts DR, Jeffries R. 2010. Logjam controls on channel:floodplain interactions in wooded catchments and their role in the formation of multi-channel patterns. *Geomorphology* **116**: 305–319.

Shields FD, Smith RH. 1992. Effects of large woody debris removal on physical characteristics of a sand-bed river. *Aquatic Conservation: Marine and Freshwater Ecosystems* **2**: 145–163.

Shroba RR, Schmidt PW, Crosby EJ, Hansen WR. 1979. *Geologic and geomorphic effects in the Big Thompson Canyon area, Larimer County*. U.S. Geological Survey Professional Paper 1115-B, Washington DC.

Spreitzer G, Tunnicliffe J, Friedrich H. 2020a. Large wood (LW) 3D accumulation mapping and assessment using structure from motion photogrammetry in the laboratory. *Journal of Hydrology* **581**: 124430.

© 2020 John Wiley & Sons, Ltd.

Spreitzer G, Tunnicliffe J, Friedrich H. 2020b. Porosity and volume assessments of large wood (LW) accumulations. *Geomorphology* **358**: 107122.

Stanford JA, Ward JV, Liss WJ, Frissell CA, Williams RN, Lichatowich JA, Coutant CC. 1996. A general protocol for restoration of regulated rivers. *Regulated Rivers: Research and Management* **12**: 391–413.

Swanson FJ, Johnson SL, Gregory SV, Acker SA. 1998. Flood disturbance in a forested mountain landscape: interactions of land use and floods. *BioScience* **48**: 681–689.

Venarsky MP, Walters DM, Hall RO, Livers B, Wohl E. 2018. Shifting stream planform state decreases stream productivity yet increases riparian animal production. *Oecologia* **187**: 167–180.

Ver Straeten CA. 2013. Beneath it all: bedrock geology of the Catskill Mountains and implications of its weathering. *Annals of the New York Academy of Sciences* **1298**: 1–29.

Wheaton JM, Brasington J, Darby SE, Sear DA. 2010. Accounting for uncertainty in DEMs from repeat topographic surveys: improved sediment budgets. *Earth Surface Processes and Landforms* **35**: 136–156.

Wohl E. 2010. *Mountain Rivers Revisited*. American Geophysical Union Press: Washington, D.C.

Wohl E. 2011. Threshold-induced complex behavior of wood in mountain streams. *Geology* **39**: 587–590.

Wohl E. 2017. Bridging the gaps: an overview of wood across time and space in diverse rivers. *Geomorphology* **279**: 3–26.

Wohl E, Cadol D. 2011. Neighborhood matters: patterns and controls on wood distribution in old-growth forest streams of the Colorado Front Range, USA. *Geomorphology* **125**: 132–146.

Wohl E, Ikeda H. 1997. Experimental simulation of channel incision into a cohesive substrate at varying gradients. *Geology* **25**: 295–298.

Wohl E, Scott DN. 2017. Wood and sediment storage and dynamics in river corridors. *Earth Surface Processes and Landforms* **42**: 5–23.

Wohl E, Lininger KB, Scott DN. 2018a. River beads as a conceptual framework for building carbon storage and resilience to extreme climate events into river management. *Biogeochemistry* **141**: 365–383.

Wohl E, Scott DN, Lininger KB. 2018b. Spatial distribution of channel and floodplain large wood in forested river corridors of the northern Rockies. *Water Resources Research* **54**: 7879–7892.

Wohl EE. 1992. Bedrock benches and boulder bars: floods in the Burdekin Gorge of Australia. *Geological Society of America Bulletin* **104**: 770–778.

Wohl EE. 1993. Bedrock channel incision along Piccaninny Creek, Australia. *Journal of Geology* **101**: 749–761.

Wolman, MG. 1954. A method of sampling coarse river-bed material. *EOS, Transactions American Geophysical Union* **35**: 951–956.

Wyzga B, Mikus P, Zawiejska J, Ruiz-Villanueva V, Kaczka RJ, Czech W. 2017. Log transport and deposition in incised, channelized, and multithread reaches of a wide mountain river: tracking experiment during a 20-year flood. *Geomorphology* **279**: 98–111.

Yellen B, Woodruff JD, Kratz LN, Mabee SB, Morrison J, Martini AM. 2014. Source, conveyance and fate of suspended sediments following Hurricane Irene, New England, USA. *Geomorphology* **226**: 124–134.

Yorks TE, Leopold DJ, Raynal DJ. 2000. Vascular plant propagule banks of six eastern hemlock stands in the Catskill Mountains of New York. *Journal of the Torrey Botanical Society* **127**: 87–93.

Supporting Information

Additional supporting information may be found online in the Supporting Information section at the end of the article.

Figure S1. Illustration of the downstream progression of erosional features in bedrock reaches of Biscuit Brook. First photo shows narrow inner channel.

Figure S2. Examples of *in-situ* and transported large wood along Biscuit Brook.

Table S1. Differences in high-water marks and modelled water-surface elevation for 5-year flow

Table S2. HEC-RAS reach-averaged shear stress values (Nm^{-2}) for subreaches in A4 at modelled discharge values

© 2020 John Wiley & Sons, Ltd.